Journal of Hazardous Materials 186 (2011) 280–287

Contents lists available at ScienceDirect

Journal of Hazardous Materials

journal homepage: www.elsevier.com/locate/jhazmat

Nano-scale metallic iron for the treatment of solutions containing multiple inorganic contaminants

T.B. Scott[a,*], I.C. Popescu[b], R.A. Crane[a], C. Noubactep[c]

[a] Interface Analysis Centre, University of Bristol, UK
[b] Research and Development National Institute for Metals and Radioactive Resources – ICPMRR, Bucharest, Romania
[c] Angewandte Geologie, Universität Göttingen, Goldschmidtstraße 3, D – 37077 Göttingen, Germany

ARTICLE INFO

Article history:
Received 6 August 2010
Received in revised form 27 October 2010
Accepted 29 October 2010
Available online 9 November 2010

Keywords:
Heavy metals
Mine water
Nanoparticles
Radionuclides
Zerovalent iron

ABSTRACT

Although contaminant removal from water using zero-valent iron nanoparticles (INP) has been investigated for a wide array of chemical pollutants, the majority of studies to date have only examined the reaction of INP in simple single-contaminant systems. Such systems fail to reproduce the complexity of environmental waters and consequently fail as environmental analogues due to numerous competitive reactions not being considered. Consequently there is a high demand for multi-elemental and site-specific studies to advance the design of INP treatment infrastructure. Here INP are investigated using batch reactor systems over a range of pH for the treatment of water containing multi-element contaminants specifically U, Cu, Cr and Mo, selected to provide site-specific analogues for leachants collected from the Lişava mine, near Oraviţa in South West Romania. Concurrently, a U-only solution was also analysed as a single-system for comparison.

Results confirmed the suitability of nano-Fe^0 as a highly efficient reactive material for the aqueous removal of Cr^{IV}, Cu^{II} and U^{VI} over a range of pH applicable to environmental waters. Insufficient Mo^{VI} removal was observed at pH >5.7, suggesting that further studies were necessary to successfully deploy INP for the treatment of geochemically complex mine water effluents. Results also indicated that uranium removal in the multi-element system was less than for the comparator containing only uranium.

1. Introduction

Due to low production costs and high efficiency for removal of a wide range of contaminants [1], metallic iron (Fe^0), is the most widely studied chemical reductant for environmental applications to date [2], and is widely used as an affordable technology for commercial soil and water remediation [3–5]. At present, Fe^0 is typically used as a reactive material in an engineered permeable reactive barrier (hereafter termed PRB), with remediative materials in the form of micro-scale powders and/or macro scale filings/granules. Such remediative methods however, in order to prevent trench failure, are limited to water treatment only at relatively shallow depths [6] precluding their use for a vast array of contaminated sites worldwide. Additional to this, such remediative materials, with relatively low surface area per unit mass, demonstrate limited reactivity for contaminant removal [7,8]. Financial, legislative and time-related constraints have therefore necessitated continued research into alternative techniques that provide a *better*, *faster* and *cheaper* cleanup. A logical development has been to scale down the reactive Fe^0 particulate to the nano-scale. Nano-Fe^0, by virtue of a minuscule size, offers a significant improvement in surface area per unit mass with subsequent improved reactivity and reaction efficacy and, additionally, offers the possibility of subsurface employment via injection. Nano-Fe^0 is therefore well poised to represent the next generation of remediation technologies, improving on cost, efficacy and versatility [7,9].

Research into contaminant removal using metallic iron has demonstrated that the remediation mechanism varies depending on the contaminant of interest [3–5,10]. Following this premise, research over the past decade has demonstrated the efficacy of nano-Fe^0 for the remediation of a wide range of contaminants including chlorinated organics, selected inorganic ions, a wide range of heavy metals and radionuclides (Ba^{II}, TcO_4^-, U^{VI}) [11–15].

The prevailing concept regarding Fe^0 as a reducing agent has been recently revisited [16,17], and regards the Fe–H_2O-contaminant system as dynamically evolving, where metallic iron (Fe^0) in aerated water (typical of meteoric and surface sources) is considered to undergo oxidative chemical transformations progressing towards an equilibrium redox state with the surrounding liquid. During this process Fe^0 is a source of aqueous Fe^{II}, Fe^{III}, H, H_2 and various precipitates (e.g. $Fe(OH)_2$, $Fe(OH)_3$, Fe_3O_4, Fe_2O_3,

* Corresponding author. Tel.: +44 0 117 3311176.
E-mail addresses: t.b.scott@bristol.ac.uk (T.B. Scott), ioana.popescu@icpmrr.ro (I.C. Popescu), richard.crane@bristol.ac.uk (R.A. Crane), cnoubac@gwdg.de (C. Noubactep).

0304-3894/$ – see front matter © 2010 Elsevier B.V. All rights reserved.
doi:10.1016/j.jhazmat.2010.10.113

Table 1
Standard electrode potentials of iron redox couples relevant for discussion of the reactivity of Fe^0 in this work: ubiquitous groundwater constituents (H^+, $O_{2(aq)}$), and four selected contaminants (CrO_4^{2-}, Cu^{2+}, MoO_4^{2-}, UO_2^{2+}). Electrode potentials are arranged in increasing order of E^0. An electrochemical reaction occurs between an oxidant of higher E^0 and a reductant of lower E^0. Therefore, under certain conditions ($E^0 < -0.44$ V) structural and organic Fe^{II} are more powerful reductants than Fe^0. All four tested elements could be reduced by Fe^0, $Fe^{II}_{(s)}$, $Fe^{II}_{(org)}$ and H^+.

Redox couple	E^0 (V) (SHE)	Eq.
$Fe^0 \rightarrow Fe^{2+} + 2e^-$	−0.44	(1)
$Fe_{(s)}{}^{2+} \rightarrow Fe_{(s)}{}^{3+} + e^-$	−0.34/−0.65	(2)
$Fe_{org}{}^{2+} \rightarrow Fe_{org}{}^{3+} + e^-$	0.52/−0.51	(3)
$2H^+ + 2e^- \rightarrow H_2$ (g)	0.00	(4)
$UO_2{}^{2+}(aq) + 2e^- \rightarrow UO_2$ (s)	0.27	(5)
$Cu^0 \rightarrow Cu^{2+} + 2e^-$	0.33	(6)
$MoO_4{}^{2-} + 4H^+ + 2e^- \rightarrow MoO_2 + 2H_2O$	0.65	(7)
$Fe^{2+} \rightarrow Fe^{3+} + e^-$	0.77	(8)
$O_2 + 2H_2O + 4e^- \rightarrow 4OH^-$	0.81	(9)
$CrO_4{}^{2-} + 8H^+ + 3e^- \rightarrow Cr^{3+} + 4H_2O$	1.51	(10)

FeOOH. green rusts) [18,19] with contaminant removal occurring in conjunction with such processes.

Contaminants are primarily removed by: (i) adsorption onto iron corrosion products (CPs); and (ii) incorporation and co-precipitation with CPs, with the further consideration that adsorbed and co-precipitated contaminants may subsequently be electrochemically transformed (oxidised or reduced). Direct interactions between Fe^0 and contaminants are therefore typically extremely limited or non-existent under most environmental water conditions. Additional to this, assuming formation and storage in a dry environment, metallic iron will possess a pre-existing surface oxide of predominantly magnetite [20,21]. Resultantly, the extent of contaminant removal depends on: (i) the pH-dependent solubility of iron; and (ii) the pH-dependent affinity of contaminants for precipitated iron corrosion products (pH at the point of zero charge – pH_{pzc}).

1.1. Context for research on more complex water systems

Although contaminant removal by Fe^0 has been extensively documented, the majority of studies have only examined single-contaminant systems. Such systems typically fail as environmental analogues due to numerous competitive reactions not being considered. Consequently there is a high demand for multi-elemental and site-specific studies for Fe^0 remediation to advance the design of treatment infrastructure. The current study is concerned with the application of nano-Fe^0 for the treatment of uranium contaminated mine water from the Lişava Valley, Banat, Romania. Preliminary laboratory analysis has determined appreciable concentrations of numerous other contaminant species, notably Cr, Cu and Mo. To further assess the suitability of nano-Fe^0 for the remediation of such multi-contaminant systems, 10 ppm solutions of Cr, Cu, Mo and U were synthesised with starting pH buffered at 3.0, 5.7, 6.8, 7.0, and 9.0. Solutions were treated with nano-Fe^0 and periodically sampled over a period of 168 h (7 days) to determine the rates and efficacy of contaminant removal, and provide direct comparison with a U^{VI}-only contaminant system.

1.2. Drivers for efficacy of contaminant removal

Cr, Cu, Mo and U are all chemically reducible by Fe^0, with standard electrode potentials listed in Table 1, and following the order of Cr ≫ Mo > Cu > U. This order however fails to take into account standard electrode potentials from chemical products formed indirectly during iron corrosion, such as dissolved Fe^{II}, adsorbed Fe^{II} and organic-complexed Fe^{II}, which have a significant bearing on the thermodynamics of contaminant removal [22–25]. With these included, the order of contaminant removal is therefore predicted to be: U > Mo > Cu > Cr (see molar weights in Table 2). This reduction efficiency series, however, further fails to take into account that at pH >4.5 Fe^0 oxidative dissolution occurs via the formation of a protective oxide layer. Therefore at pH >4.5, the efficiency of Fe^0 for contaminant removal primarily depends on the affinity of the contaminant for in-situ formed iron oxide, which is dependent upon electrical transfer between the soluble contaminant and the protective oxide layer.

Table 2
Molar ratio nano-Fe^0:contaminant (n_{Fe}/n_{ct}) used in the present study. The volume of the contaminated solution was 500 mL with 10 mg L^{-1} starting concentration for each contaminant.

Element	Mass (g/mol)	Concentration		n_{Fe}/n_{ct}
		(mg L^{-1})	(μM)	
Cr	52.00	10	192.3	46.6
Cu	63.55	10	157.4	56.9
Mo	95.94	10	104.2	85.9
U	238.03	10	42.0	213.1
Fe^0	55.85	500	8952.6	1.0

Furthermore, the process via which contaminants are removed as a function of pH can be categorised into two hypotheses. The first assumes that the Fe^0–H_2O system is a reducing system, with an order of removal efficiency of Cr ≫ Mo > Cu > U. The second assumes that the Fe^0–H_2O system is primarily an adsorptive system and the extent of contaminant removal depends on the solubility of the contaminants and their relative affinity to corrosion products; in this case removal efficiency would follow U > Mo > Cu > Cr.

The present study has therefore been established not only to determine the rates of efficacy for contaminant removal by nano-Fe^0 but to also determine the predominant mechanism for contaminant removal in complex multi-elemental solutions.

2. Materials and methods

2.1. Chemicals

All chemicals (iron sulphate ($FeSO_4{\cdot}7H_2O$), sodium hydroxide (NaOH), sodium borohydride ($NaBH_4$), nitric acid (HNO_3), hydrochloric acid (HCl), potassium hydrogen phthalate ($KHC_8H_4O_4$), potassium dihydrogen phosphate (KH_2PO_4), sodium tetraborate ($Na_2B_4O_7$), uranyl(VI) acetate ($UO_2(CH_3COO)_2$), molybdenum(VI) dichloride dioxide (MoO_2Cl_2), copper(II) chloride ($CuCl_2$), chromium(VI) chloride ($CrCl_6$), potassium chromate (K_2CrO_4) and solvents (ethanol, acetone) used in this study were of analytical grade and all solutions were prepared using Milli-Q water (resistivity >18.2 MΩ cm).

2.2. Nanoparticle synthesis

Iron nanoparticles were synthesised following an adaptation of the method first described by Wang and Zhang [7], using sodium borohydride to reduce ferrous iron to a metallic state via the following reaction:

$$2Fe^{2+} + BH_4{}^- + 3H_2O \rightarrow 2Fe^0\downarrow + H_2BO_3{}^- + 4H^+ + 2H_2$$

Briefly, 7.65 g of $FeSO_4{\cdot}7H_2O$ was dissolved in 50 mL of Milli-Q water (>18.2 MΩ cm) and then a 4 M NaOH solution was used to adjust the solution pH to 6.8. The salts were reduced to metallic nanoparticles by the addition of 3.0 g of $NaBH_4$. The nanoparticle product was isolated through centrifugation and then sequentially washed with water, ethanol and acetone (20 mL of each). The nanoparticles were dried in a dessicator under low vacuum (approx 10^{-2} mbar) for 48 h and then stored in the oxygen-free nitrogen environment of a Saffron Scientific glovebox until required.

Table 3
Solution pH buffer reagent parameters used to adjust system pH values. Each solution was then made up with 10 ppm Cr, Cu, Mo and U and up to 500 mL with Milli-Q water (resistivity >18.2 MΩ cm).

pH	Primary pH buffer reagent	Secondary pH buffer reagent
3	5.105 g $KHC_8H_4O_4$	111.5 mL of 0.1 M HCl
5.7	1.021 g $KHC_8H_4O_4$	19.85 mL of 0.2 M NaOH
6.6	0.680 g KH_2PO_4	8.87 mL of 0.2 M NaOH
7.0	3.405 g KH_2PO_4	72.75 mL of 0.2 M NaOH
9.0	2.385 g $Na_2[B_4O_5(OH)_4]\cdot 8H_2O$	23 mL of 0.1 M HCl

The starting particulate was characterised using X-ray photoelectron spectroscopy (XPS), X-ray diffraction (XRD), electron microscopy (SEM/TEM) and surface area analysis (BET method).

2.3. Experimental methodology

Ten 500 mL solutions of 10 mg L^{-1} Cr^{VI}, Cu^{II}, Mo^{VI}, U^{VI} were prepared using chromium(VI) chloride ($CrCl_6$), copper(II) chloride ($CuCl_2$), molybdenum(VI) dichloride dioxide (MoO_2Cl_2) and uranyl(VI) acetate ($UO_2(CH_3COO)_2$) respectively and held in sealed high density polyethylene (HDPE) containers. Two batches of solutions (one for INP exposure and one to act as a control) were each adjusted to pH values of 3.0, 5.7, 6.8, 7.1 and 9.0 using 0.1 M HCl and NaOH. Potassium hydrogen phthalate, potassium dihydrogen phosphate and sodium tetraborate were used as primary salts to buffer the solutions, see Table 3 for concentrations. A further set of U-only pH buffered solutions were also prepared at 10 mg L^{-1} U concentration to provide comparison for the multi-contaminant systems.

To each system, 0.25 g of nano-Fe^0 was added and experimental sampling was conducted at 0, 3, 6, 9, 12, 24, 48 and 168 h. Prior to sampling, batch reactors were gently shaken to ensure homogeneity and then aliquots of 25 mL were taken. The extracted solution samples were filtered through a 0.22 μm cellulose acetate filter into a 50 mL centrifuge tube and a drop of concentrated HNO_3 was added to prevent sorption to the vessel walls prior to further preparation for atomic absorption spectroscopy (AAS) and photocolorimetry.

Experiments were performed in sealed batch reactors in the open laboratory to maintain levels of dissolved oxygen (hereafter termed DO) close to that measured in waters collected from settling ponds at the Lişava mine (Banat, Romania) (7–9 mg L^{-1}). Measurements of both pH and ORP were made using a CONSORT C832 multi-parameter analyser with a combined pH-ORP probe head. Dissolved oxygen concentrations were measured using a Jenway 970 DO_2 meter probe.

2.4. Aqueous concentration analysis

Liquid samples were prepared for AAS analysis by a 10 times dilution in 1% nitric acid (analytical quality concentrated HNO_3 in Milli-Q water). Blanks and standards for analysis were also prepared in 1% nitric acid, with Fe, Cu and Cr standards of 0.10, 0.25, 0.50, 1.00, 2.5, 5.0 and 10.0 ppm. A Varian 220 AAS spectrometer was used for solution analysis of Fe, Cu and Cr. Photocolorimetry was used to determine the solution concentrations of U and Mo, using a Cecil CE1101 photocolorimeter at wavelengths 670 nm and 490 nm respectively.

2.4.1. Expression of experimental results

After determining the residual aqueous concentration of the contaminant elements (C), the corresponding percent removal (P) was calculated according to the following equation:

$$P = [1 - (C/C_0)] \times 100\%$$

Table 4
Variation of pH ($\Delta pH = pH_{final} - pH_{initial}$) in the investigated systems as a function of time. The largest pH variation ($\Delta pH = 1.3$) was noticed in the multi-element system with an initial pH of 5.7.

Time (h)	pH 3.0	pH 5.7	pH 6.8	pH 7.0	pH 9.0
Single-element system (U^{VI})					
0	0.0	0.0	0.0	0.0	0.0
3	0.3	0.3	0.2	0.1	0.0
6	0.6	0.5	0.3	0.1	0.2
9	0.7	0.5	0.5	0.1	0.0
12	0.5	0.3	0.5	0.2	0.0
24	0.3	0.4	0.6	0.2	0.0
48	0.5	0.6	0.8	0.3	0.0
168	0.6	0.6	1.2	0.4	0.0
Multi-element system (Cr^{VI}, Cu^{II}, Mo^{VI}, U^{VI})					
0	0.0	0.0	0.0	0.1	0.0
3	0.1	0.5	−0.2	0.0	0.1
6	0.4	1.0	0.0	−0.1	0.0
9	0.3	1.3	0.1	0.0	0.0
12	0.2	1.3	0.7	0.2	−0.1
24	0.6	1.3	0.3	0.2	−0.1
48	0.5	1.2	0.5	0.3	−0.1
168	−0.1	0.9	1.1	0.1	0.0

C_0 is the initial aqueous contaminant concentration (about 10 mg L^{-1}) and C gives the concentration after the experiment. The operational initial concentration (C_0) for each sampling time was acquired from a triplicate control experiment without nano-Fe^0 (so-called blank). This procedure was to account for element adsorption onto the walls of the reaction vessels, element precipitation due to over-saturation and all other possible side reactions during the experiments.

For discussion purposes, weight concentrations (mg L^{-1}) were converted into molar concentration (mmol L^{-1} or μmol L^{-1}) and the number of moles (μmoles) of each element derived by known equations.

3. Results and discussion

3.1. pH and Eh variation

pH and Eh results as a function of reaction time for single and multi-elemental systems are compiled in Tables 4 and 5, with minimal pH variation observed for all systems and minimal Eh variation observed after 3 h reaction time following a significant rapid ini-

Table 5
Final redox potential (Eh) in the investigated systems as function of time. In all the systems, the initial Eh value (about 230 mV) decreases to approximately −200 mV and then varies within ±15 mV.

Time (h)	pH 3.0	pH 5.7	pH 6.8	pH 7.0	pH 9.0
Single-element system (U^{VI})					
0	+246	+241	+229	+217	+232
3	−197	−201	−200	−206	−198
6	−196	−203	−205	−204	−187
9	−195	−188	−193	−205	−188
12	−195	−196	−200	−203	−196
24	−197	−200	−199	−195	−195
48	−198	−193	−199	−194	−195
168	−200	−205	−198	−195	−200
Multi-element system (Cr^{VI}, Cu^{II}, Mo^{VI}, U^{VI})					
0	+238	+223	+226	+221	+211
3	−194	−194	−199	−189	−192
6	−195	−197	−202	−212	−202
9	−193	−197	−195	−183	−196
12	−189	−196	−195	−194	−194
24	−195	−195	−197	−196	−192
48	−197	−195	−198	−198	−196
168	−193	−196	−196	−207	−192

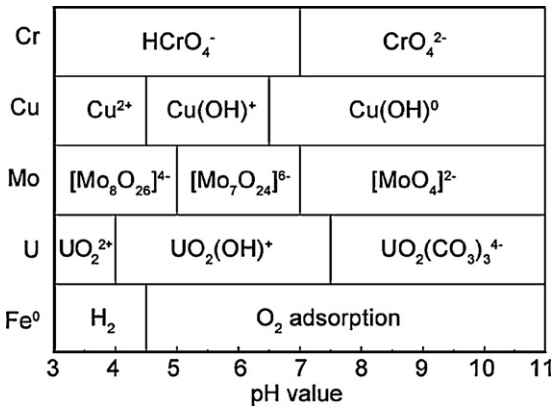

Fig. 1. Schematic representation of the pH dependence of the type of metallic iron (Fe^0) oxidative dissolution and the speciation of the four investigated elements. To investigate all possible figures, the initial pH was varied from 3.0 to 9.0. A too rapid pH increase as result of intensive nanoparticles dissolution was avoided by moderately the solutions.

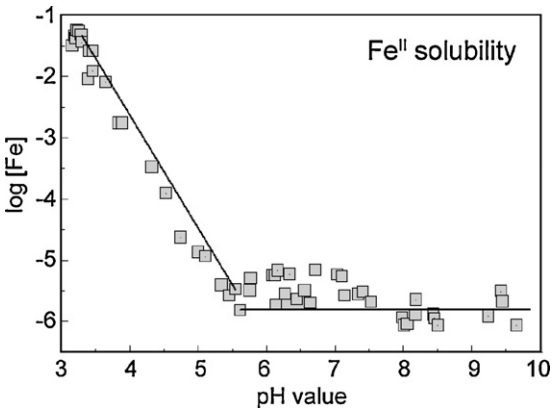

Fig. 2. pH-dependent solubility data for Fe^{II} in 0.1 M NaCl (25 °C) [33]. The trend is the same as for the oxidative dissolution of Fe^0 as discussed in the text. Below approximately pH 5.5 Fe^{II} solubility is direct proportional to pH. Above pH 5.5, Fe^{II} remains relatively constant at about 10^{-6} M. The lines are not fitting functions; they connect points to facilitate visualisation.

tial decrease in Eh from ~+230 mV at zero time to ~−200 mV at 3 h.

Maximum pH variation ($\Delta pH = pH_{final} - pH_{initial}$) observed for single and multi-systems, was 1.2 and 1.3 pH units for the pH 6.8 single-system and pH 5.7 multi-system respectively. An average pH variation of 0.35 and 0.40 was observed for single and multi-system respectively. Following the addition of nano-Fe^0, Eh variation ($\Delta Eh = Eh_{final} - Eh_{3\ h}$) observed for single and multi-systems, was on average <±15 mV (Table 4), which is within the range of expected experimental errors [26].

This insignificant change observed in pH highlights the validity of using buffers to maintain the pH at a constant value for better description of the processes occurring during contaminant removal by nano-Fe^0. It should, however, be kept in mind that the measured pH and Eh values are that of the bulk solution which is not necessarily a true reflection of the conditions in the immediate vicinity the nanoparticle surfaces. The significant decrease in Eh values by more than 400 mV attests to the capacity of nano-Fe^0 to rapidly change oxic to anoxic conditions through the consumption of dissolved oxygen and production of hydrogen through hydrolysis. However, it should also be recognised that although solution Eh can have a profound effect on contaminant solubility [33], chemical reduction does not explicitly imply contaminant removal. For example, the chemical reduction of Cr^{VI} at pH 3 by Fe^{II} yields soluble Cr^{III} which is observed to only precipitate at solution pH >6 [27,28]. For the purpose of the following discussion O_2 consumption will be referred to as being synonymous with decreasing Eh.

3.2. Effect of pH on iron solubility

The corrosion of iron as a function of pH is well documented in the literature; see [29–32] for reviews. At approximately pH >4.5, iron oxidative dissolution is considered to occur primarily via the reduction of dissolved oxygen (Table 1; Eq. (9)) with the formation of anionic, hydroxo species (Fig. 1). Within the range of 4.5 < pH < 10, due to the low solubility of Fe^{II}, iron dissolution is observed as relatively constant as a function of pH (Fig. 2) [33]. Fig. 3 compares the solubility of Fe^{II} and Fe^{III} recorded by [33] and [34] respectively with the final iron concentration measured in this study. It can be seen that measured concentrations are close to, or higher than, Fe^{II} solubility. This behaviour is ascribed to the high reactivity of nano-Fe^0 yielding a meta-stable (over saturated) Fe^{II} solution, and clearly indicates the significance of pH in controlling the magnitude of iron oxidative dissolution (Fig. 2). It also is important to note that, irrespective of pH, an equilibrium exists between iron dissolution and iron precipitation. Therefore, the measured aqueous concentration of iron may not provide a true reflection of the dynamics of these systems. To gain a better idea of the pH-dependent Fe^0 reactivity, the evolution of the changes in dissolved oxygen concentration for each system was examined.

3.3. Effect of pH on O_2 consumption

Fig. 4 contrasts DO consumption as a function of reaction time for single (Fig. 4A) and multi-element (Fig. 4B) systems at initial pH 3.0, 5.7 and 9.0. In these systems DO consumption is ascribed to two different redox processes: (i) Fe^0 oxidation to Fe^{II}; and (ii) Fe^{II} oxidation to Fe^{III}, with the measured dissolved O_2 recording a balance between oxygen consumed by the nano-Fe^0, through the formation of CPs, and oxygen recharge from the atmosphere. With atmospheric dissolution/diffusion considered constant for all batch reaction systems, variations in DO consumption and recovery can therefore be directly attributed to differential rates of CP formation and dissolution, occurring as a function of Fe^{II} solubility, which itself is controlled by solution pH (Fig. 2).

Fig. 4 displays that, in all systems, during the first 12 h of reaction, rapid and significant DO consumption was observed. For pH 3.0 and 5.7 this initial period of DO consumption is followed by a period of gradual recovery in DO concentrations attributed to atmospheric ingress. This was observed as most significant with low solution pH and less effective in the multi-contaminant system.

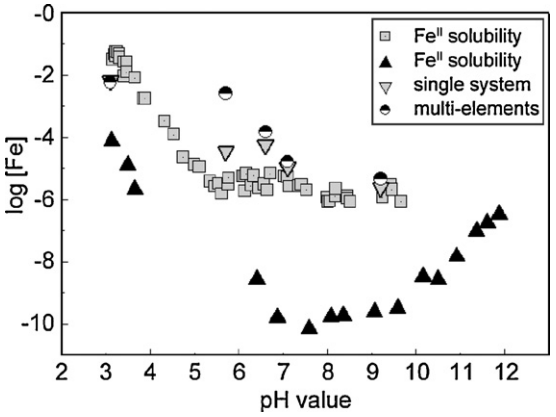

Fig. 3. pH-dependent solubility data for Fe^{II} and Fe^{III} recorded by Rickard [33] and Liu and Millero [34] respectively with the final iron concentration measured in this study.

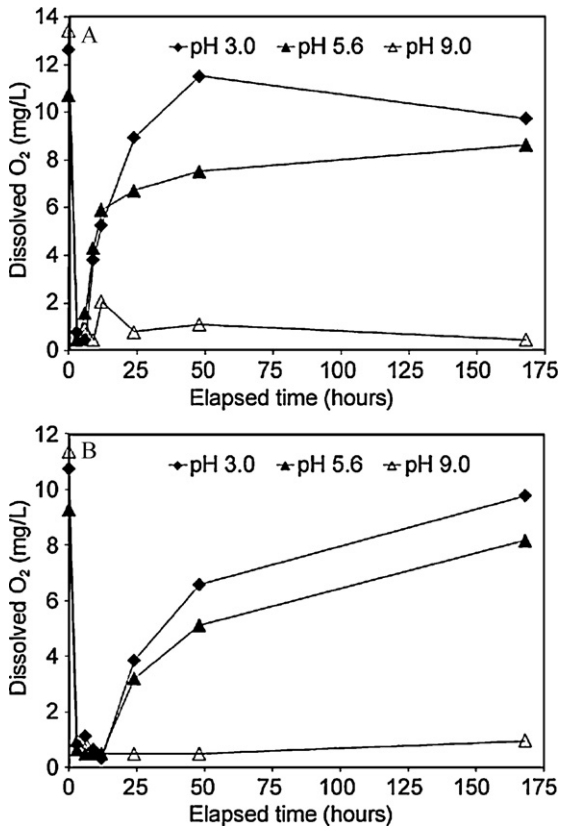

Fig. 4. (A) Dissolved oxygen (mg L^{-1}) as a function of reaction time (h) for starting pH values of 3.0, 5.7 and 9.0 for the single-contaminant system. (B) Dissolved oxygen (mg L^{-1}) as a function of reaction time (h) for starting pH values of 3.0, 5.7 and 9.0 for the multi-contaminant system.

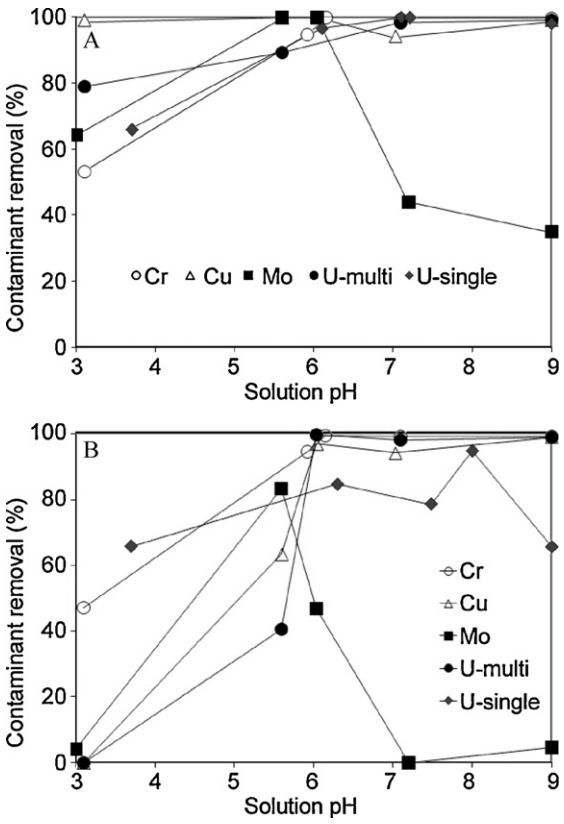

Fig. 5. (A) Maximum observed contaminant removal (%) versus system pH. (B) Contaminant removal (%) as a function of pH for 168 h reaction time.

At pH 3.0, Fe^{II} and Fe^{III} solubility is high (Fig. 3), and the rapid DO recovery observed is ascribed to limited CP formation. Simply put, Fe is more stable in an aqueous state. At pH 5.7, Fe^{II} and Fe^{III} solubility is significantly less (Fig. 3), by more than 4 orders of magnitude, but interestingly the recovery of DO concentrations was observed to be similar to the system at pH 3. This is attributed to the impairment of Fe^0 corrosion via the formation of a physical CP barrier between the metal and the surrounding aqueous media. At pH 9.0, Fe^{II} solubility remains relatively constant, however Fe^{III} solubility is further reduced (Fig. 3). Consequently the lack of DO recovery observed in this reaction system can be attributed to the significant formation of Fe^{III} corrosion products at high solution pH [35].

Additional to a reduction in iron solubility between pH 5.7 and 9.0, the differential consumption in DO observed might also be partially attributed to the net electrochemical charge of the nanoparticle surfaces. As solution pH for the different systems span either side of the PZC for CPs ($5.7 < (CP)_{pzc} < 9.0$), surfaces are positively and negatively charged respectively. Therefore as DO is electronegative, oxygen scavenging is more effective for the positively charged surfaces, and resultantly low DO recovery in the pH 9.0 system can be partially ascribed to the effective promotion of oxic complexes by the positively charged nanoparticle surfaces.

To summarise, rapid initial DO consumption in all systems is attributed to the rapid formation of CPs. Following this initial phase, DO recovery at starting pH of 3.0 and 5.7 is attributed to the effect of CP in providing a physical barrier that limits continued corrosion of the nano-Fe^0 surfaces by preventing direct interaction of Fe^0 with the surrounding aqueous media. At pH 9.0 the formation of CPs is observed as more continuous, with CP growth limited by the rate of O_2 ingress from the atmosphere. The slower recovery in DO levels observed in the multi-contaminant systems relative to the single-contaminant systems is attributed to the presence of a greater mass of dissolved metals.

3.4. Effect of pH on contaminant removal

Fig. 5A displays maximum observed contaminant removal for single and multi-elemental systems as a function of pH. The results can be summarised as follows: (i) at pH <4 Cu is the only contaminant with >90% removal; (ii) at 5.7 < pH < 7 for at least one sampling time all contaminants were observed with >90% removal; and (iii) at pH ≥7 Mo removal fails to exceed 50%. Results therefore concur with previous work that Fe^0, as a remediative technology, is appropriate for treatment of contaminated waters at pH >4.5 only [16,18,19]. Additional to this, as <50% Mo removal was observed at pH ≥7, results suggest that a complimentary remediative material will be required for Mo-contaminated mine water treatment using Fe^0.

Fig. 5B can be used to determine the mechanism of contaminant removal as a function of pH (discussed in Section 1.2). The following order of contaminant removal can be established: (i) pH 3.0: $Cr \gg Mo > Cu \approx U$; (ii) pH 5.9: $Cr > Mo > Cu > U$; (iii) pH 7.0: $Cr \approx U > Cu \gg Mo$; and (iv) pH 9.0: $Cu \approx Cr \approx U \gg Mo$.

The observed behaviour indicates that at pH ≤5.7 contaminant removal conforms to a chemically reductive model (see Section 1.2), whilst at higher pH (>5.7) removal conforms to neither the aforementioned reductive or adsorptive model systems. It is therefore considered that the observed uptake behaviour observed at pH 7 and pH 9 is more complex than initially postulated. It should be acknowledged that in all systems, regardless of pH, rapid initial adsorption of contaminants onto the INP surfaces was observed within the first few hours of reaction. Subsequently, at pH ≤5.7 sorbed contaminants become proportionally chemically reduced (forming a precipitate) through coupled redox reactions with Fe^{II}

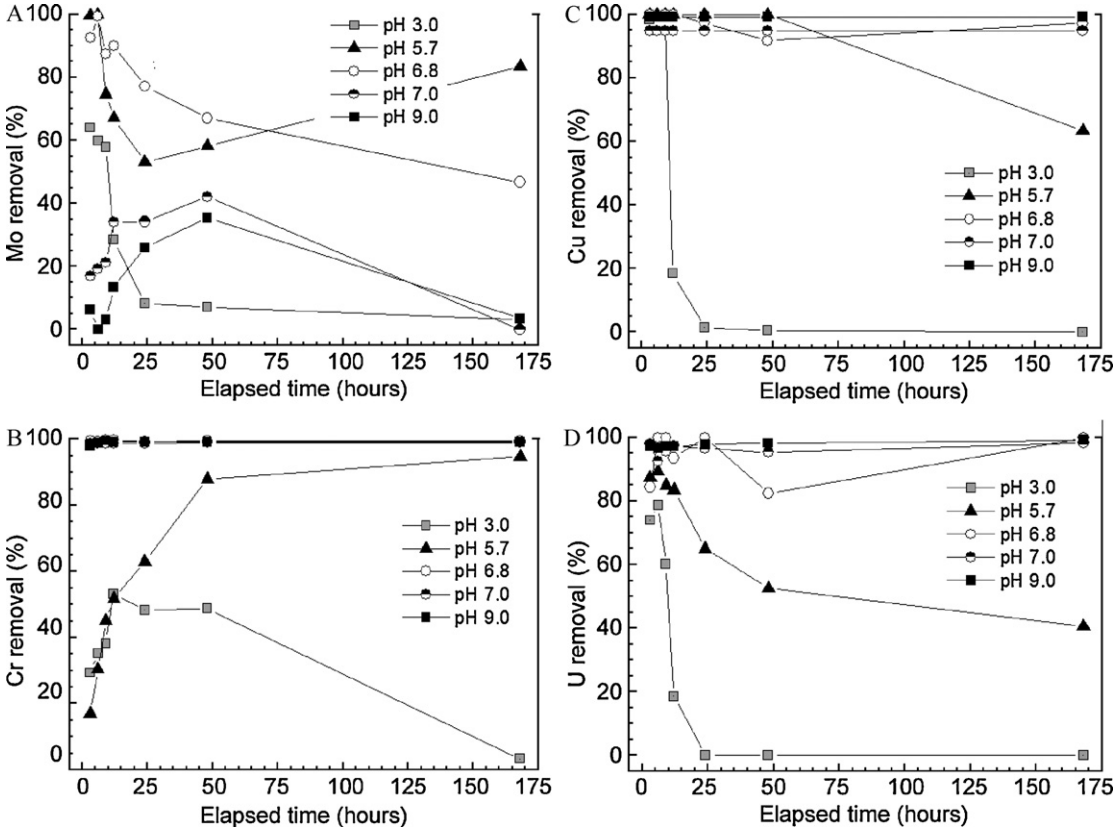

Fig. 6. (A) Mo^{VI} removal (%) as a function of reaction time (h) and starting pH. (B) Cr^{VI} removal (%) as a function of reaction time (h) and starting pH. (C) Cu^{II} removal (%) as a function of reaction time (h) and starting pH. (D) U^{VI} removal (%) as a function of reaction time (h) and starting pH.

and following expected thermodynamic order. At pH >5.7 the observed uptake reflects both: (i) the relative aqueous solubility of each contaminant and, (ii) the competition between reductive precipitation and structural incorporation into forming CPs as mechanisms for removal, with the latter mechanism considered to increasingly predominate at higher pH and contaminant concentrations [36].

3.4.1. Mo removal using nano-Fe^0

As a contrast to Cr^{VI}, Cu^{II} and U^{VI}, maximum removal of Mo^{VI} (Fig. 6A) was observed in the systems with initial pH 5.7 and 6.8. Mo^{VI} removal is observed as insignificant at pH 3.0 and for pH $\geq$7.0, with no appreciable Mo^{VI} removal observed after 168 h of reaction (Fig. 6A). This differential behaviour is ascribed to Mo being increasingly insoluble with decreasing solution pH [37–40], ascribed to polymerisation into successively less soluble higher molecular weight oxide complexes (Fig. 4). Fig. 1 also shows that: dependent on pH, the speciation of the contaminants varies, indicating that under variable pH conditions applicable for the environment (6.0 < pH < 9.0) anionic and/or cationic contaminant complexes may be present and accordingly the mechanisms for removal may vary.

Based on the current results successful removal of all four contaminants using nano-Fe^0 may only be achieved in water systems where pH remains at approximately 6.0 for the duration of the reaction. This is highly unlikely for most environmental waters but can be achieved in ex-situ contaminant removal systems where the pH can be successfully buffered, however for in-situ applications (such as subsurface injection) nano-Fe^0 will not provide a complete remediation solution. The application of a PRB remediative system may however prove appropriate for Mo^{VI} cleanup using Fe^0, with removal via size exclusion [15]. Alternatively, a complimentary material such as MnO_2 could be added adjacent to the Fe^0 bed.

3.5. Time dependent contaminant removal

Fig. 6 displays contaminant removal in the multi-element system as a function of time. It can be observed that for elements Cr, Cu and U removal efficiency follows the order 3.0 < 5.7 < 6.8 ≈ 7.0 ≈ 9.0, with maximum U and Cu removal obtained at the first sampling time (3 h) for all pH conditions studied, and maximum removal of Cr for solution pH >5.7 after 12 h and 168 h respectively. Maximum Mo removal was observed after 3 h for pH 3.0, 6 h for pH of 5.7 and 6.8, and after 48 h for pH of 7.0 and 9.0.

As discussed in the previous section, at pH ≤5.7 chemical reduction is considered to be the prevalent mechanism of contaminant removal (following an initial sorption step). However, as pH decreases the solubility of Cr, Cu and U increase, which dictates that less contaminant removal occurs and accounts for the low contaminant removal observed at pH <4.0. Maximum removal was therefore observed for solution pH >5.7 with removal of Cr^{VI}, Cu^{II} and U^{VI} observed as >90% for all timescales. Given the low solubility of Fe at pH >6.0, contaminant removal is ascribed to the adsorptive affinity of contaminants with iron corrosion products, with adsorbed and enmeshed contaminants possibly further reduced by adsorbed Fe^{II}, adsorbed H/H_2 or Fe^0 [17,41,42].

3.5.1. Comaprison of U removal for single and multi-elemental systems

A major difference observed between the single and multi-element systems is the overall ionic strength, which may in part explain the observed differences in uranium uptake. The calculated molar ratio of iron to contaminants in both systems yields

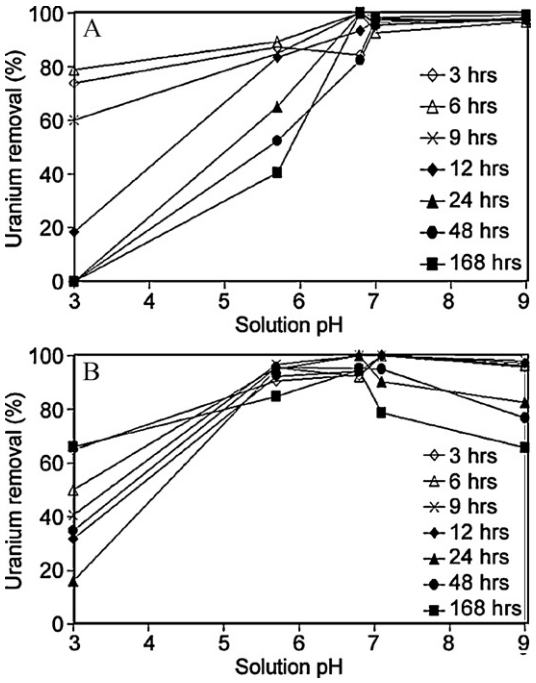

Fig. 7. (A) U^{6+} removal as a function of pH and reaction time (h) for the multi-contaminant system. (B) U^{6+} removal as a function of pH and reaction time (h) for the single-contaminant system.

values of 17.9 and 212.6 for the multi- and single-contaminant systems respectively. Whilst both systems conceptually have a reactive excess of Fe, only a portion of it is expected to be available for contaminant interactions at the INP surfaces, with the rest being protected by CPs. Consequently in the multi-element systems, direct and close competition between contaminants for surface sorption sites is considered to have occurred and resultantly (Fig. 7) less effective uranyl removal is observed in the multi-contaminant system for pH conditions pH $\leq$6.8, which may also have been aided by the formation of highly soluble stable mixed contaminant complexes.

As a contrast however, for pH conditions >6.8, the multi-element system exhibited no significant uranium re-dissolution by 168 h reaction time, which was in contrast to the U-only system. This can be attributed to the stability of contaminants in the solid phase being more significant for a higher ionic strength solution. Further work is required in order to elucidate this theory.

4. Concluding remarks

The present work has demonstrated nano-Fe^0 as highly suitable for efficient removal of contaminants Cr^{VI}, Cu^{II} and U^{VI} for a wide range of pH conditions and timescales, despite any competing reactions that may have occurred. The following key conclusions can be drawn:

1. For pH conditions appropriate to environmental waters (pH >5.7) average removal after 7 days reaction time was 99%, 96% and 99% respectively, for aqueous Cr^{VI}, Cu^{II} and U^{VI}.
2. Appreciable removal of Mo^{VI} however was only observed for pH conditions more acidic than found in environmental waters, with an average removal efficiency of <5% after 7 days reaction time for systems at pH >5.7.
3. In all reactive systems, the dissolution of iron from the nanoparticle surfaces was observed, with rapid uptake of dissolved oxygen indicating the formation of CPs.

From the current study it is not clear to what extent CPs are involved in contaminant removal or whether the mechanism of removal is the same for each contaminant. At low pH ($\leq$5.7) the data indicates that the primary pathway for contaminant removal and retention is via adsorption and subsequent chemical reduction. However, at pH >5.7 the responsible mechanisms are not readily determined. Consequently future research is required on surface modification techniques and complimentary materials analysis to elucidate the mechanisms via which contaminants such as Mo^{VI}, with low affinities to iron corrosion products, can be successfully removed from solution by nano-Fe^0.

Whilst recognising that the aqueous systems investigated in the current work do not have the complexity of environmental waters, the current work on uranium remediation has also demonstrated that single contaminant laboratory test systems will provide an overestimate for removal with respect to waters with more complex chemistry. Additionally, the data presented for the multi-element test systems provide some indication that the increased ionic strength of environmental samples may well contribute to improved long-term performance for remediation using INP, through extended immobilization of the target contaminants. Further experiments on selected environmental solutions containing uranium will seek to examine this hypothesis.

Acknowledgments

We would like to thank NATO for supporting this work through the Science for Peace, Cooperative Science and Technology Sub-Programme.

References

[1] R. Miehr, P.G. Tratnyek, J.Z. Bandstra, M.M. Scherer, M. Alowitz, E.J. Bylaska, Diversity of contaminant reduction reactions by zerovalent iron: role of the reductate, Environ. Sci. Technol. 38 (2004) 139–147.
[2] P.G. Tratnyek, M.M. Scherer, T.J. Johnson, L.J. Matheson, Permeable reactive barriers of iron and other zero-valent metals, in: M.A. Tarr (Ed.), Chemical Degradation Methods For Wastes And Pollutants: Environmental and Industrial Applications, Marcel Dekker, New York, 2003, pp. 371–421.
[3] A.B. Cundy, L. Hopkinson, R.L.D. Whitby, Use of iron-based technologies in contaminated land and groundwater remediation: a review, Sci. Total Environ. 400 (2008) 42–51.
[4] A.D. Henderson, A.H. Demond, Long-term performance of zero-valent iron permeable reactive barriers: A critical review, Environ. Eng. Sci. 24 (2007) 401–423.
[5] M.M. Scherer, S. Richter, R.L. Valentine, P.J.J. Alvarez, Chemistry and microbiology of permeable reactive barriers for in situ groundwater clean up, Rev. Environ. Sci. Technol. 30 (2000) 363–411.
[6] R.W. Puls, Permeable reactive subsurface barriers for the interception and remediation of chlorinated hydrocarbon and chromium(VI) plumes in groundwater. U.S. EPA Remedial Technology Fact Sheet, (1997) http://www.epa.gov/nrmrl/pubs/600f97008/600f97008.pdf – date accessed 11/05/10.
[7] C.B. Wang, W.X. Zhang, Synthesizing nanoscale iron particles for rapid and complete dechlorination of TCE and PCBs, Environ. Sci. Technol. 31 (1997) 2154–2156.
[8] C. Macé, S. Desrocher, F. Gheorghiu, A. Kane, M. Pupeza, M. Cernik, P. Kvapil, R. Venkatakrishnan, W.X. Zhang, Nanotechnology and groundwater remediation: A step forward in technology understanding, Remediation 16 (2006) 23–33.
[9] W.X. Zhang, Nanoscale iron particles for environmental remediation: an overview, J. Nanopart. Res. 5 (2003) 323–332.
[10] S.F. OïHannesin, R.W. Gillham, Long-term performance of an in situ "iron wall" for remediation of VOCs, Ground Water 36 (1998) 164–170.
[11] D.W. Blowes, C.J. Ptacek, S.G. Benner, W.T. Mcrae Che, T.A. Bennett, R.W. Puls, Treatment of inorganic contaminants using permeable reactive barriers, J. Contam. Hydrol. 45 (2000) 123–137.
[12] K.J. Cantrell, D.I. Kaplan, T.W. Wietsma, Zero-valent iron for the in situ remediation of selected metals in groundwater, J. Hazard. Mater. 42 (1995) 201–212.
[13] M. Dickinson, T.B. Scott, The application of zero-valent iron nanoparticles for the remediation of a uranium-contaminated waste effluent, J. Hazard. Mater. 178 (2010) 171–179.
[14] S.J. Morrison, D.R. Metzler, B.P. Dwyer, Removal of As, Mn, Mo, Se, U, V and Zn from groundwater by zero-valent iron in a passive treatment cell: reaction progress modelling, J. Contam. Hydrol. 56 (1–2) (2002) 99–116.
[15] S.J. Morrison, P.S. Mushovic, P.L. Niesen, Early breakthrough of molybdenum and uranium in a permeable reactive barrier, Environ. Sci. Technol. 40 (6) (2006) 2018–2024.

[16] C. Noubactep, Processes of contaminant removal in "Fe^0–H_2O" systems revisited. The importance of co-precipitation, Open Environ. J. 1 (2007) 9–13.
[17] C. Noubactep, A critical review on the mechanism of contaminant removal in Fe^0–H_2O systems, Environ. Technol. 29 (8) (2008) 909–920.
[18] C. Noubactep, The suitability of metallic iron for environmental remediation, Environ. Prog. 29 (3) (2010) 286–291.
[19] C. Noubactep, A. Schöner, P. Woafo, Metallic iron filters for universal access to safe drinking water, Clean 37 (2009) 930–937.
[20] M. Odziemkowski, Spectroscopic studies and reactions of corrosion products at surfaces and electrodes, Spectrosc. Prop. Inorg. Organomet. Compd. 40 (2009) 385–450.
[21] T.B. Scott, M. Dickinson, R.A. Crane, O. Riba, G.M. Hughes, G.C. Allen, The effects of vacuum annealing on the structure and surface chemistry of iron nanoparticles, J. Nanopart. Res. 12 (5) (2010) 1765–1775.
[22] J.P. Gould, The kinetics of hexavalent chromium reduction by metallic iron, Water Res. 16 (1982) 871–877.
[23] A.F. White, M.L. Peterson, Reduction of aqueous transition metal species on the surfaces of Fe(II)-containing oxides, Geochim. Cosmochim. Acta 60 (20) (1996) 3799–3814.
[24] J.T. Strathmann, T.A. Stone, Reduction of oxamyl and related pesticides by Fe^{II}: influence of organic ligands and natural organic matter, Environ. Sci. Technol. 36 (23) (2002) 5172–5183.
[25] D. Naka, D. Kim, T.J. Strathmann, Abiotic reduction of nitroaromatic compounds by aqueous iron(II)-catechol complexes, Environ. Sci. Technol. 40 (9) (2006) 3006–3012.
[26] B.J. Merkel and B. Planer-Friedrich, Praxisorientierter leitfaden zur modellierung von beschaffenheit, kontamination und sanierung aquatischer systeme, *Grundwasserchemie Springer Verlag*, 220 (2002), S. 74 Abb., 56 Tab., mit CD-ROM. ISBN: 3-540r-r42836-4.
[27] L.Y. Chang, Alternative chromium reduction and heavy metal precipitation methods for industrial wastewater, Environ. Prog. 22 (3) (2003) 174–182.
[28] L.Y. Chang, Chromate reduction in wastewater at different pH levels using thin iron wires – A laboratory study, Environ. Prog. 24 (3) (2005) 305–316.
[29] A.Y. Aleksanyan, A.N. Podobaev, I.I. Reformatskaya, Steady-state anodic dissolution of iron in neutral and close-to-neutral media, Prot. Met. 43 (1) (2007) 66–69.
[30] S. Nesic, Key issues related to modelling of internal corrosion of oil and gas pipelines–A review, Corros. Sci. 49 (2007) 4308–4338.
[31] G.W. Whitman, R.P. Russel, V.J. Altieri, Effect of hydrogen-ion concentration on the submerged corrosion of steel, Ind. Eng. Chem. 16 (2) (1924) 665–670.
[32] E.R. Wilson, The Mechanism of the corrosion of iron and steel in natural waters and the calculation of specific rates of corrosion, Ind. Eng. Chem. 15 (2) (1923) 127–133.
[33] D. Rickard, The solubility of FeS, Geochim. Cosmochim. Acta 70 (2006) 5779–5789.
[34] X. Liu, F.J. Millero, The solubility of iron hydroxide in sodium chloride solutions, Geochim. Cosmochim. Acta 63 (1999) 3487–3497.
[35] J.R. Rustad, K.M. Rosso, A.R. Felmy, Molecular dynamics investigation of ferrous–ferric electron transfer in a hydrolyzing aqueous solution: calculation of the pH dependence of the diabatic transfer barrier and the potential of mean force, J. Chem. Phys. 120 (16) (2004) 7607–7615.
[36] T.B. Scott, G.C. Allen, P.J. Heard, A.C. Lewis, D.F. Lee, The extraction of uranium from groundwaters on iron surfaces, Proc. R. Soc. 461 (2057) (2005) 1247–1259.
[37] K.Z. Elwakeel, A.A. Atia, A.M. Donia, Removal of Mo(VI) as oxoanions from aqueous solutions using chemically modified magnetic chitosan resins, Hydrometallurgy 97 (1–2) (2009) 21–28.
[38] K.P. Saripalli, B.P. McGrail, D.C. Girvin, Adsorption of molybdenum on to anatase from dilute aqueous solutions, Appl. Geochem. 17 (5) (2002) 649–656.
[39] J.A.M. van den Berg, Y. Yang, H.H.K. Nauta, A. van Sandwijk, M.A. Reuter, Comprehensive processing of low grade sulphidic molybdenum ores, Miner. Eng. 15 (11) (2002) 879–883.
[40] Z. Zhao, G. Zhang, G. Huo, H. Li, Kinetics of atmospheric leaching molybdenum from metalliferous black shales by air oxidation in alkali solution, Hydrometallurgy 97 (3–4) (2009) 233–236.
[41] A. Ghauch, H.A. Assi, S. Bdeir, Aqueous removal of diclofenac by plated elemental iron: bimetallic systems, J. Hazard. Mater. 182 (1–3) (2010) 64–74.
[42] A. Ghauch, H.A. Assi, A. Tuqan, Investigating the mechanism of clofibric acid removal in Fe^0/H_2O systems, J. Hazard. Mater. 176 (2010) 48–55.